INTERACTION OF DNA AND RNA MOLECULES WITH NANOCLAYS THAT HAVE POTENTIAL FOR USE IN GENE THERAPY

by

Archana Gujjari, M.S.

A dissertation submitted to the Graduate Council of
Texas State University in partial fulfillment
of the requirements for the degree of
Doctor of Philosophy with a Major in
Material Science, Engineering and Commercialization
December 2017

Committee Members:

Gary Beall, Chair

L. Kevin Lewis, Co-Advisor

Ben Martin

William Chittenden

Clois E. Powell

COPYRIGHT

by

Archana Gujjari

2017

FAIR USE AND AUTHOR'S PERMISSION STATEMENT

Fair Use

Duplication Permission

ACKNOWLEDGEMENTS

I would sincerely like to thank my research advisors and mentors Dr. Gary Beall and Dr. Kevin Lewis who provided me an opportunity to join their team and for providing access to the laboratory and research facilities. Their guidance, patience and motivation helped me in all the time of research and writing of dissertation. I would like to thank my dissertation committee Dr. Clois E Powell, Dr. William Chittenden and Dr. Ben Martin for their insightful comments. I am extremely thankful for my lab mates Blanca Rodriguez, Shubha Malla, Monica Weis, Angelica Riojas and friends at Texas State University Akila, Neha, Mounica and Shruthi for their encouragement. I am grateful for my husband Kiran Kumar Nalla and his family for their love and support which has always motivated me to push myself and to reach my goals. I am also grateful to my parents Gujjari Srinivas and Gujjari Anitha and my family members Ashwini and Sairam for all their motivation throughout my education and career. I would like to dedicate my dissertation to my beloved husband and my parents. None of this would have been possible without them.

TABLE OF CONTENTS

Page

LIST OF FIGURES

Figure **Page**

ABSTRACT

In recent years, research has been carried out in the field of drug/biomolecule delivery for optimizing the carrier. Nanoclays such as halloysite (HNT) and montmorillonite (MMT) can be used as protective carriers for drug/biomolecule delivery. Halloysites are naturally occurring aluminosilicate clay nanotubes. Montmorillonite (MMT) forms sheet-like structures with large surface areas. Both the clays have been utilized successfully as vehicles for delivery of drugs into cells. In the current study, we have investigated the association of RNAs and DNAs having different structures and lengths with HNT and MMT using physical and molecular biology methods. The strength of MMT-ssRNA interactions was also examined using inorganic anion competition and displacement assays.

In this study, we have demonstrated that small single-stranded and double-stranded DNAs and RNAs have little affinity for the nanoclay HNT. However, addition of Na^+ and Mg^{2+} cations increased binding of the nucleic acids to HNT. The nature of DNA bound to HNT and the ability of HNT to protect DNA from nuclease DNase I was also investigated. The strength of the interaction between small RNAs and Ca-MMT was also assessed using anion competition and displacement experiments as well as electrophoretic mobility shift assays. The anion competition and displacement experimental data suggested that binding of RNAs to the clay was strong and was not disrupted significantly by the inorganic counterions.

CHAPTER I

INTRODUCTION

Background

Gene therapy is becoming a promising treatment option for cancer and genetic disorders. The main objective of gene therapy is to deliver foreign genetic material into specific cell types or tissues by using efficient and non-toxic gene carriers. Using gene therapy scientists can inject, edit or delete specific bits of DNA or RNA in patient cells. Inserted genes can inactivate or knock down improperly functioning genes and can also introduce a normal copy of a gene into cells that lack one. Thus, gene therapy could be a promising treatment option for a number of diseases without using drugs or surgery. In order to inject the genes into a patient's body, a protective carrier is needed. DNA and RNA are vulnerable to chemical and enzymatic degradation and cannot penetrate through cell membranes easily when administered into a human body (1). In order to deliver genes, various vectors such as cationic polymers, lipids and viral vectors are being utilized as gene carrier systems; each has its own limitations (2). A brief summary of how gene therapy works is shown in Figure 1(3).

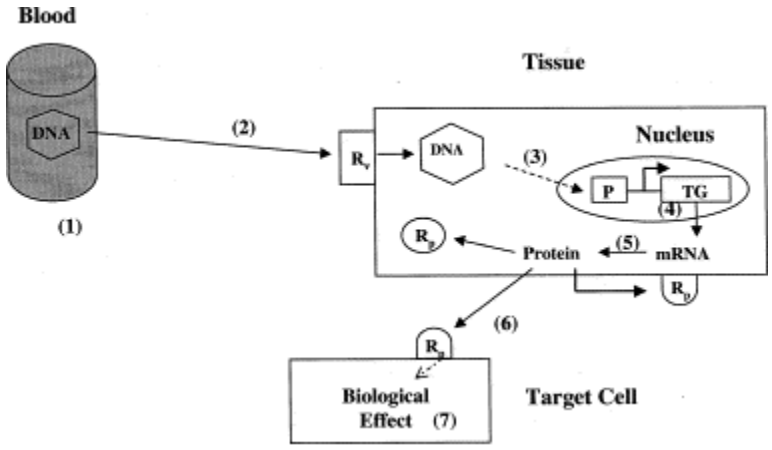

Figure 1. Steps involved in biological process of *in vivo* gene transfer. (1) Introduction of vector (viral, non-viral, cell-based) into body via bloodstream or direct tissue injection; (2)

Identification of target tissue by vector through specific receptors (Rv) present on target tissue cells; (3) Vector enters the cytoplasm to reach and enter the nucleus to deliver vector DNA or therapeutic gene; (4) The therapeutic gene participates in transcription to form mRNA in the nucleus; (5) mRNA is translated into therapeutic protein in the cytoplasm; (6) The therapeutic protein interacts with receptors (Rp) within the producing cell (intracrine mechanism) or on the surface of producing cell (autocrine mechanism) or on neighboring cells (paracrine mechanism) or at distant sites from the target tissue after entering blood circulation (endocrine mechanism) (e.g., erythropoietin, coagulation factors, growth hormone, etc.); (7) After the therapeutic protein interacts with its receptor, it induces an appropriate biological effect which results in therapeutic benefits[3].

Gene therapy vehicles can be categorized mainly into two groups: viral vectors and non-viral vectors. Approximately 80% of 210 gene therapy protocols that have been approved for phase 1 clinical trials utilized virus vectors (4). Viral vectors are naturally evolved from viruses that are capable of transferring their genetic material into host cells. The viruses used in gene therapy are modified to eliminate their pathogenicity. An example of viral vector gene therapy is shown in Figure 2 (5).

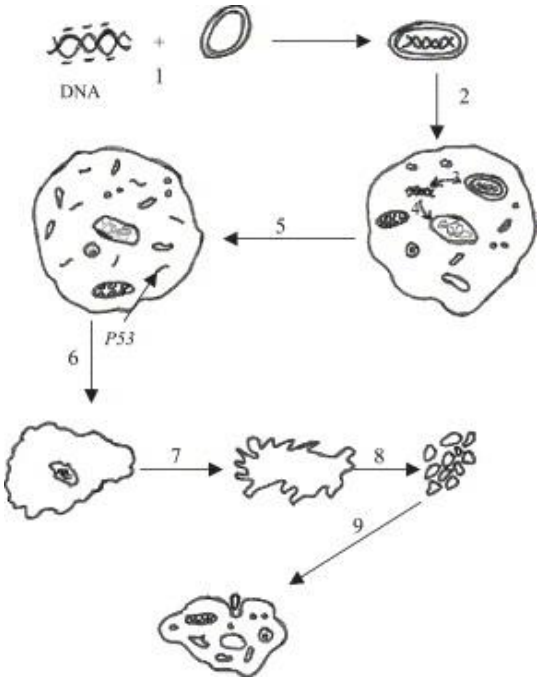

Figure 2. Schematic representation of viral vector gene therapy for restoration of the activity of p53 gene in p53 gene-mutated or deficient tumors. (1) p53 DNA is encapsulated in suitable gene carrier (adenovirus or retrovirus); (2) DNA/carrier complex reaches the targeted cells; (3)

Release of DNA in the cytoplasm; (4) DNA enters the nucleus; (5) Production of p53 protein; (6) Shrinkage of cell and condensation of chromosomes occurs; (7) Membrane bubbling; (8) Induces Apoptosis; (9) Phagocytosis and digestion of apoptotic bodies by neighboring cells[5].

Though viral vectors successfully transport genes to the host cell without degradation, they have certain disadvantages. The viruses can usually infect more than one type of cell. They might infect healthy cells as well as cancer cells. Sometimes the desired/new gene might be inserted in the wrong location, which could result in harmful mutations. For example, in clinical trials for X-linked severe combined immunodeficiency (X-SCID), in which the hematopoietic stem cells were transduced with a corrective gene using a retrovirus vector, the treatment led to the development of T cell leukemia in 4 of 20 patients (6). If the viral vectors are unintentionally introduced into patient's reproductive cells, it could produce changes that may be passed to offspring. Sometimes the transferred gene may be overexpressed, producing an excess of missing protein which might cause an immune reaction. Viral vectors also have limitations in terms of the size of the inserted genetic materials. These limitations are encountered less frequently with non-viral vectors, but non-viral vectors are less efficient than viral vectors.

Examples of non-viral gene delivery systems include direct DNA delivery, liposomes and DNA-protein complexes, each having its own advantages and limitations. Non-viral vectors are generally cationic in nature and they interact with negatively charged DNA through electrostatic interactions. However, the net charge is positive, which enables the carrier to efficiently interact with negatively charged cell membranes and internalize into the cell by endocytosis. An example of non-viral (synthetic) vector gene therapy is shown in Figure 3 (7).

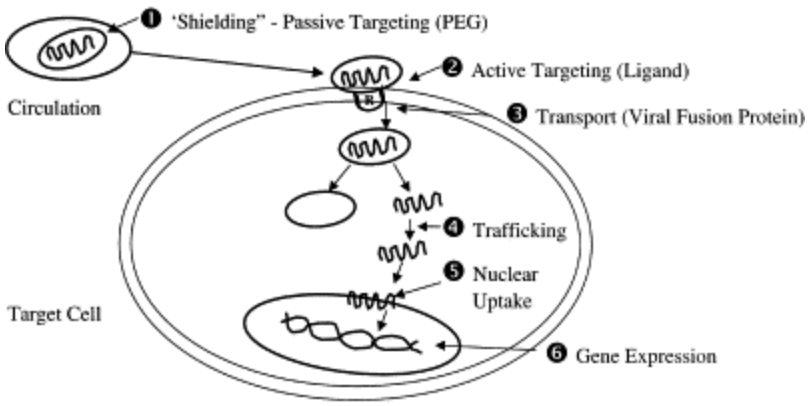

Figure 3. Non-viral vector gene delivery process. DNA is densely packed with synthetic materials such as protamine sulfate and the surface is shielded (e.g., by polyethylene-glycol [PEG]) to prevent from binding to plasma proteins, blood cells or to each other and to allow longer circulating plasma half-life. (1) uptake in target tissues (e.g., at the site of leaky vessels in tumors) ("passive" targeting). The surface of the particles is engineered with specific ligands for targeting to selected cells/tissues; (2) Entry into the cell via cell recognition ligands, cell membrane fusion proteins and nuclear localization signals; (3) Cellular trafficking and prevention of intracellular degradation of DNA; (4) uptake of therapeutic gene into nucleus facilitated by viral nuclear localization signal (NLS) peptides; (5) Chromosomal localization and insertion allowing for long-term expression of the therapeutic gene; (6) Gene expression (7).

Both viral and non-viral gene delivery systems suffer from specific types of shortcomings. The main advantages and disadvantages of different gene delivery systems are summarized in Table 1. There is a necessity to develop a safe and effective vector system for delivering genes into target cells and tissues without detrimental side effects. Protective gene carriers that have great promise are nanoclays.

Table 1. Summary of advantages and disadvantages of different gene delivery systems (8).

Strategy	Method	Pros	Cons
Naked DNA or RNA	Direct injection *in vivo*	Simplicity of production and use Potential use as genetic vaccines	Low efficiency Transitory effect Internalization only in skeletal and cardiac myocytes and in antigen presenting cells
Physical methods	Electroporation	Relatively easy to set up for skeletal muscle and skin; invasive for other organs	Low efficiency Transitory effect Limited spectrum of applications
	Increase of hydrodynamic pressure	Usually invasive	Low efficiency Transitory effect
	Ultrasounds (sonoporation)	Relatively easy to set up	
	Bombardment with DNA-coated gold particles (gene gun)	Relatively easy to set up Stimulation of an effective immune response	Limited to gene transfer to the skin
	Jet injection		
Chemical methods	Liposomes Cationic lipids Cationic polymers Proteins	Relatively easy to set up and use	Relatively low efficiency Transitory effect
Viral vectors	Vectors based on: gammaretroviruses, lentiviruses, adenoviruses, adeno-associated viruses (AAVs), herpesviruses	High efficiency of gene transfer both *in vivo* and *ex vivo* For some vectors, persistence of therapeutic gene expression *in vivo*	Possible induction of immune and/or inflammatory response Limited cloning capacity Complexity of production For some viruses, tropism limited to specific cell types Insertional mutagenesis (for gammaretroviruses) In most cases, incomplete knowledge of the molecular mechanisms governing viral replication

Nanoclays

Nanoparticles are defined as particles having ≤100 nm in at least one dimension (9-12). Nanoclays are defined as clay minerals whose particles are in nanoscale dimensions. These are

tiny crystalline substances evolved primarily from chemical weathering of certain rock-forming minerals. Although clays belong to wider group of minerals, in chemistry they can be simply described as hydrous silicates. Clays can be found abundantly in nature or can be synthesized easily in a lab. Because of their environmentally friendly nature, low cost, and availability in nature, nanoclay studies are gaining importance in different applications in biomedicine (13-17). Clays can be classified into four major groups: the kaolinite group, montmorillonite/smectite group, illite group, and the chlorite group (18).

Nanoclays have sheet-like geometry and are referred to as phyllosilicates (19-22). Fundamental units of clay minerals include silica tetrahedra and aluminum octahedra which are depicted in Figure 4. These units are held together by ionic bonds. The silica tetrahedron consists of a central silicon atom surrounded by four oxygen atoms arranged in tetrahedral coordination. The combination of tetrahedral silica units gives a silica sheet. Three oxygen atoms at the base of the tetrahedron are shared by a neighboring tetrahedron. The octahedral unit consists of an aluminium or magnesium ion bound by six oxygens or hydroxyl groups arranged in the form of an octahedron and the combination of the octahedral aluminum hydroxyl units gives an octahedral sheet.

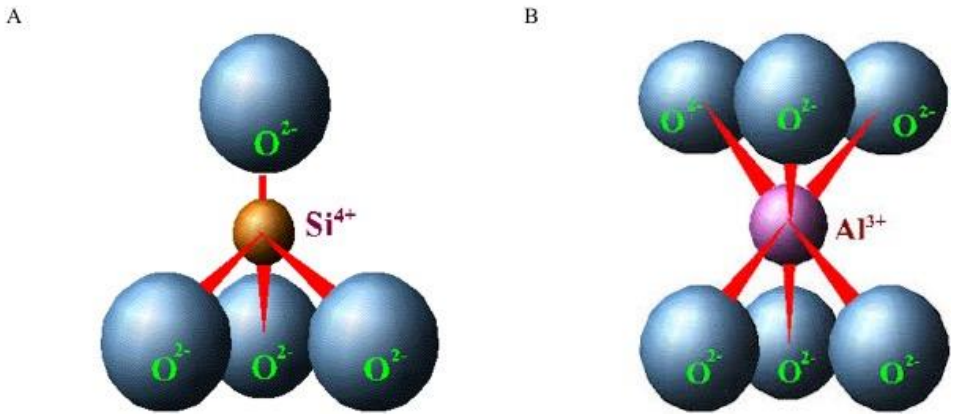

Figure 4. Schematic representation of Silicon tetrahedron and Aluminium octahedral structure of Nanoclays. A) Silicon tetrahedron structure showing a silicon ion in coordination with four oxygen ions to form a tetrahedral structure. B) Aluminium octahedral structure showing aluminium in coordination with six oxygen ions (23).

Based on the arrangement of tetrahedral and octahedral sheets, many clay minerals can be classified as 1:1 (having one tetrahedral and one octahedral sheet per clay layer) or 2:1 (containing two tetrahedral sheets and one octahedral sheet sandwiched between the two tetrahedral sheets) (Figure 5).

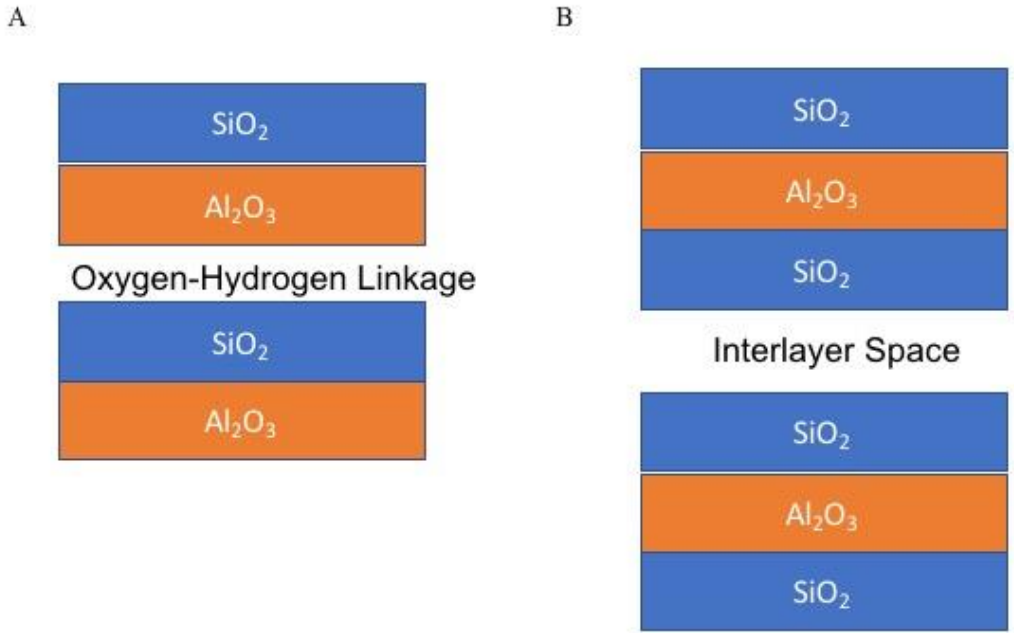

Figure 5. Structure of two different types of clay. A) kaolinite (1:1 type clay) B) montmorillonite (2:1 type clay)

The clay particles carry a net negative charge on their surfaces. Isomorphous substitution in a clay mineral is the major reason for the net negative charge on the clay particle surface. For example, replacement of Si^{4+} in tetrahedral coordination with an Al^{3+} atom and replacement of Al^{3+} by Mg^{2+} or Fe^{2+} atoms in octahedral coordination creates a shortage of positive charge, which appears as negative charge on the clay surface (24). The functional groups such as O^{2-} and OH^- present at the edges and the basal surfaces can also contribute negative charge. The other sources of charge on clay colloids are exposed hydroxyl groups (OH^-) present on the surface and the broken oxygen bonds present at the edges. The small Al^{+3} and Si^{+4} atoms may be lost due to weathering and the remaining oxygen ions have an unsatisfied net negative charge, e.g.

$>SiOH^{2+}$ <……..> $>SiOH <……..> > SiO^+ H^-$

$>AlOH^{2+}$ <……..> $>AlOH <……..> > AlO^+ H^-$

Due to the presence of net negative charge, the clay minerals attract cations and dipolar molecules such as water. Isomorphous substitution in clay minerals produces the capacity in clay sheets to hold positive charges, which is described as cation exchange capacity (CEC) (25).

Halloysite

Halloysite (HNT) is a cylindrical aluminosilicate clay mineral that occurs naturally (26). The chemical formula of HNT is $Al_2(OH)_4Si_2O_5 \cdot nH_2O$. HNT consists of a 1:1 aluminosilicate layer with abundant Si-OH and Al-OH groups. It is chemically similar to kaolinite but differs in having a hollow tubular structure (Figure 6) (27-28). The walls of HNT are composed of 10-15 bilayers of aluminum and silicon dioxide. A single layer of water is present between the unit layers. The basal spacing between the layers for hydrated halloysite is approximately 1.01 nm and 0.72 nm for dehydrated halloysite. Halloysite is tubular shaped while it is hydrated and there

is no interlayer swelling. Halloysite nanotubes have a luminal diameter of approximately 15 nm and the outside diameter ranges from 50 to 70 nm. The length of HNT particles ranges between 500 and 2000 nm. The outer surface of HNT is made up of silica while the alumina layer is confined to the inner surface (29). HNT is positively charged on the inner surface and negatively charged on the outer surface. Due to different dielectric and ionization properties of silicon and aluminium oxide, the outer and inner surfaces of HNT are oppositely charged in water at pH values ranging from 3 to 8 (30) . The above structural and chemical properties identify HNT as a green and ideal nanocarrier for drug delivery.

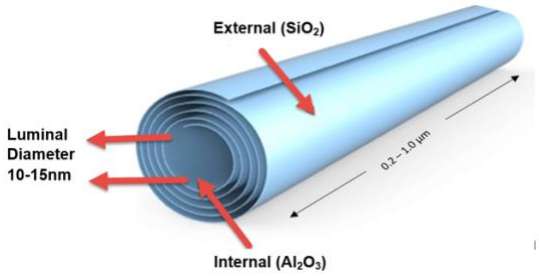

Figure 6. Structure of halloysite nanotube (31).

Montmorillonite

The general formula for the chemical structure of montmorillonite (MMT) is $M_x(Al_{2-y}Mg_y)Si_4O_{10}(OH)_2{*}nH_2O$ (32). Montmorillonite is a 2:1 type of clay containing tetrahedral sheets of silicate layers sandwiching an octahedral aluminum oxide/hydroxide layer ($Al_2(OH)_4$) (Figure 7). Montmorillonite exists as sheets and is typically hundreds of nm wide and 1 nm in thickness, with an average surface area of approximately 700 m^2/g (33). The negative charge of MMT is primarily due to extensive isomorphous substitution for aluminum by other cations such as Mg^{2+}. Montmorillonite belongs to the smectite clay group. The smectite clays can swell and expand upon hydration causing stacking, or tactoid formation, to occur. The

interlayer spacing of MMT is based upon level of hydration. Water molecules and cations exist between unit layers and the basal spacing is from 0.96 nm to infinity (after swelling).

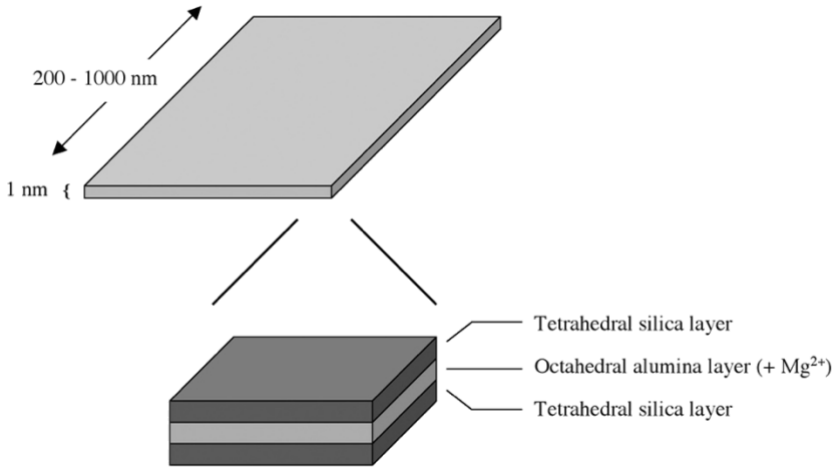

Figure 7. Layered structure of montmorillonite.

Importance of Clays

Nanoclays are being considered as potential candidates for drug and biomolecule delivery into target cells because of the following features.

1. Nanoclays are small in size and can easily traverse physiological boundaries

2. They are considered safe and are categorized as GRAS (Generally Recognized As Safe) by the FDA

3. They are inexpensive and proven to have few toxic effects

4. They do not activate the immune system

The cations present in the interlayer space of nanoclays play an important role in interaction with biomolecules. These cations can interact with negatively charged groups on drugs and biomolecules, which could be a protective strategy to shield them from chemical and enzymatic degradation. Studies related to drug loading capabilities, release characteristics and

control of the duration of release through end tube capping with polymers have been done using halloysite nanotubes. HNT demonstrated successful delivery of anti-tumor, anti-inflammatory and anti-microbial drugs (34). Elumai *et al.* pointed out the importance of diameter and length, together with particle charge, of HNT on loading and release of drugs (35) . HNT interactions with cells and subsequent intracellular uptake have been studied in different cell lines (36-38). Campos *et al*. successfully demonstrated the transfer of naked DNA using halloysite nanotubes in bovine embryos (39). Shi *et al.* demonstrated that the HNT could efficiently improve intracellular delivery and enhance the antitumour activity of antisense oligodeoxynucleotides (40).

The interaction between clay and DNA has been well studied using montmorillonite (41-42). Franchi *et al.* examined montmorillonite as a novel vector for oral gene delivery. These results indicated that montmorillonite protected plasmid DNA from the acidic environment in the stomach and DNA-degrading enzymes in the intestine, and successfully delivered it into cells of the small intestine (43). Lin *et al.* modified MMT with cationic hexadecyl trimethyl ammonium bromide (CTAB) to increase the interlayer space of the clay so that it can accommodate more DNA molecules (44).

Aims of this Project

The purpose of this study was to bring insight into the binding interactions of halloysite and montmorillonite with small DNAs and RNAs. Results of these experiments can be used to develop improved assays for quantitating the binding of larger DNAs and RNAs to clay surfaces. The approaches used here can be generally applicable to study the interaction of nanoclays with

many other biomolecules and biopolymers. The data from this research will contribute to the field of biomedicine in the context of gene therapy. Specific aims are listed below.

Aim 1 - Analyze the association of DNA and RNA molecules with halloysite nanotubes (HNT) using physical and biochemical methods. These experiments included (a) determining the optical and sedimentation properties of HNT nanotubes in aqueous solutions (b) assessing the interactions of HNT with small DNAs and RNAs having different conformations (e.g., single-stranded DNA (ssDNA), double-stranded DNA (dsDNA) and single-stranded (ssRNA)), and (c) applying physical and molecular biology approaches including co-sedimentation assays and scanning electron microscopy (SEM) to investigate the binding affinity of nucleic acids for HNT.

Aim 2 - Determine the site of binding of DNA to HNT. We hypothesized that the RNA and DNA will enter into the lumen of HNT and bind to the inner walls and will be protected from chemical and enzymatic degradation.

Aim 3 – Complete a study of the interaction between RNAs and MMT initiated by Blanca Rodriguez in the Lewis and Beall labs. These experiments included (a) assessing the strength of RNA:MMT interactions using anion displacement and competition binding assays with at least two distinct anions, sodium carbonate (Na_2CO_3), and sodium sulfate (Na_2SO_4), (b) studying the effect of heat and sonication on separation of CaMMT tactoids into individual platelets with greater surface area, and (c) use of electrophoretic mobility assays (EMSAs).

CHAPTER II

MATERIALS AND METHODS

Materials

Powdered halloysite was purchased from Naturalnano (West Henrietta, NY). Powdered homoionic sodium montmorillonite (Na-MMT) was obtained from Southern Clay Products, Inc. (Gonzalez, TX). Oligonucleotides such as DNA and RNA: ssDNA 25mer Pvu4a (AAATGAGTCACCCAGATCTAAATAA), its complement cPvu4a (TTATTTAGATCTGGGTGACTCATTT), ssRNA 25mer PvuRNA (AAAUGAGUCACCCAGAUCUAAAUAA), and its complement cPvuRNA (UUAUUUAGAUCUGGGUGACUCAUUU) were purchased from Integrated DNA Technologies (Coralville, IA). The low MW DNA Ladder and dsRNA ladder were purchased from New England Biolabs (Ipswich, MA). Eppendorf tubes (1.5 mL) were purchased from Eppendorf (Hauppauge, NY). Electrophoresis experiments were performed by using 11 x 14 cm Horizon gel rigs (Labrepco). Amersham/GE Healthcare EPS 601 was used as source of power supply. Boric acid was purchased from JT Baker (Center Valley, PA). Tris base, magnesium chloride, calcium chloride, sodium chloride, sodium carbonate and sodium sulfate were purchased from Sigma-Aldrich. Agarose was purchased from Gold Biotechnology (St. Louis, MO). SYBR Gold was obtained from Invitrogen Life Sciences (Grand Island, NY).

UV-Vis Spectrophotometric Analysis

A Cary 100 Bio UV-Vis spectrophotometer or a BioRad SmartSpec 3000 spectrophotometer was used for spectroscopic absorbance measurements and scanning of HNT and MMT samples. A 1.5 mL quartz cuvette was used for UV spectra measurements. Three

forms of HNT: untreated (unsonicated and non-vacuumed) HNT, vacuumed HNT and sonicated HNT at a concentration of 100 μg/mL in double-deionized water (ddH_2O) were scanned from 200-800 nm. Concentration-dependent spectroscopy scans of HNT samples (1000 μg/mL, 500 μg/mL, 250 μg/mL, 125 μg/mL, 100 μg/mL, 50 μg/mL and 25 μg/mL) were performed and their absorbances at 260 nm were plotted into a best fit trendline using Microsoft Excel to generate a standard line and equation. HNT samples were sonicated using a Vibracell VC501 Sonicator from Sonics & Materials (Newton, CT) at an amplitude of 60 using 3 mm probe tip for 4 min. All assays were performed for three forms of HNT (untreated, sonicated and vacuumed) using three replicates and results were averaged.

Double-stranded DNA Preparation

To make double-stranded DNA in the presence of Tris, aliquots of Pvu4a and cPvu4a of 30,000 ng each were combined, Tris (pH 7.5) was added (5 mM final), and solutions were mixed in a total volume of 200 μL to a final dsDNA concentration of 300 ng/μL. For dsDNA of final concentration 300 ng/μL in the absence of Tris, aliquots of Pvu4a and cPvu4a of 30,000 ng each were combined in a total volume of 200 μL. The solutions were heated in a heating block for 5 min at 95 ˚C and then allowed to anneal while cooling down to room temperature (RT) for 30 min. Using gel electrophoresis with 3.0% agarose and 0.5X Tris borate (TB) buffer, successful formation of dsDNA was confirmed (45). The gels were run at 200V for 30 min and stained with ethidium bromide for about 15 min. Low molecular weight (MW) DNA ladder (New England Biolabs) was run in the gel with dsDNA samples.

Double-stranded DNA (dsDNA) for MMT assays was prepared by mixing 1,050 ng Pvu4a with 1,050 ng cPvu4a plus ddH_2O and 5 mM Tris (pH 7.4) in a total volume of 1 mL for a total of 2,100 ng dsDNA.

Determining Optimum Centrifugation and Incubation Time for HNT Oligonucleotide Binding Assays

a) Centrifugation Time

Three sets for each untreated, vacuumed and sonicated solutions at different concentrations of HNT 1 mg/mL, 0.5 mg/mL, 0.25 mg/mL and 0.125 mg/mL in ddH_2O in a total volume of 1mL were prepared. The solutions were centrifuged at 25,000 xg, at 20°C for 5 min, 15 min, 30 min and 60 min. After centrifugation, the supernatant was collected and the A_{260} was measured.

b) Incubation Time

For incubation time experiments, stock solutions of 8 mg/mL HNT (untreated, vacuumed and sonicated) and 1.84 mg/mL ssDNA were prepared in ddH_2O and aliquoted to achieve final concentrations of 4 mg/mL and 33 μg/mL, respectively. Samples were mixed and incubated with continuous shaking for 5, 15 and 30 min and centrifuged for 30 min at 25,000 xg, at 20°C. The top 60 μL of the supernatant was transferred to a microcuvette for determination of absorbance at 260 nm. An A_{260} of 1.0 corresponds to a concentration of 33 μg/ml for ssDNA (46). Using this relationship, the ssDNA concentration in the supernatant and the amount of ssDNA bound to HNT was calculated.

Preparation of DNA and RNA/halloysite Solutions for Adsorption Assays

HNT-ssDNA adsorption assays with vacuumed and unvacuumed HNT solutions were performed to test the effect of vacuum in removal of trapped gases in binding oligonucleotide to HNT. The binding affinities of ssDNA, dsDNA and ssRNA 25mers to HNT at different concentrations were tested by adding oligonucleotide to increasing concentrations of HNT and the percentage of nucleic acid bound was plotted against HNT concentration. HNT-ssDNA solutions were prepared by mixing 75 µL of HNT of (8 mg/mL, 4 mg/mL, 2 mg/mL, or 1 mg/mL), 10 µL Pvu4a DNA (for a final A_{260} = 1) and ddH_2O in a final volume of 150 µL. For dsDNA, 20 µL of 406 ng/µL was added to the dsDNA/HNT solutions. HNT-RNA binding mixtures were prepared by mixing 75 µL of HNT (8 mg/mL, 4 mg/mL, 2 mg/mL or 1 mg/mL), 4.3 µL PvuRNA (for a final A_{260} = 1) and ddH_2O in a final volume of 150 µL. Each HNT centrifugation assay required a set of control tubes. Control tubes were prepared by mixing 75 µL of HNT and 75 µL ddH_2O. Salt experiment control tubes consisted of 75 µL HNT and 0.1, 1, 10, or 100 mM NaCl/$MgCl_2$ and up to 150 µL ddH_2O final volume. Assay mixtures were shaken for 15 min and centrifuged. Precipitation of clay and clay-DNA/RNA complexes was done by centrifugation at 21,000 x g for 30 min at 20 ˚C.

DNA/HNT and RNA/HNT Adsorption Analysis

The top 60 µL of the supernatant was transferred into a new tube immediately after centrifugation and the A_{260} was measured. The percentage of DNA or RNA bound to HNT could be calculated by subtracting the absorbance of the supernatant (unbound nucleic acid to HNT) from the original nucleic acid-only absorbance and dividing the resulting value by the original nucleic acid-only absorbance. The average of three to five samples for each DNA-HNT and

RNA-HNT series was calculated. Microsoft Excel software was used for graphical analysis of the centrifugation results.

HNT-DNA-Nuclease Experiment

Extraction of DNA bound to clay particles is difficult (47-48) as DNA strands bind tightly to the clay (49-51). Heating DNA could potentially be used as one of the techniques for DNA recovery. To determine whether HNT would be a suitable carrier in gene therapy, the nature of DNA recovered after binding to HNT was determined from the following experiment. Adsorption of DNA on to HNT was made by mixing 225 µL of HNT (4 mg/mL), 8.1 µL of cPvu4a ssDNA (474 ng/ µL), 45 µL of $MgCl_2$ (100 mM) and ddH_2O in a final volume of 450 µL. The adsorption process was run by shaking the tubes at room temperature in a vortex mixer (Fisher Scientific) for 15 min, followed by centrifugation of clay and clay plus DNA pellet at 25,000 xg for 30 min at 20 ˚C. The supernatant was discarded and the pellet was washed twice with two volumes of ddH_2O.

The pellet obtained after centrifugation was resuspended in 19 µL ddH_2O. Then 2 µL of 10x DNase buffer, 1 µL of DNase I was added and the tube was incubated for 10 min at 37 ˚C for nuclease reaction. The enzyme reaction was terminated by heating the mixtures in the tube at 98 ˚C for 5 min. Later 7.5 µL of 30% glycerol was added to tubes and 22 µL of it was loaded on to a gel. Control HNT-ssDNA-$MgCl_2$ solutions were prepared as described above except without addition of nuclease and DNase buffer. Control ssDNA/nuclease was prepared by mixing 3 µL ssDNA (47.4 ng/µL), 23 µL ddH_2O, 3 µL 10x DNase buffer and 1 µL DNase I and incubation for 10 min at 37 ˚C. A control ssDNA tube contained 3 µL ssDNA (47.4 ng/µL) + 7 µL TE + 3 µL dye. Gel electrophoresis was performed using 0.5X TB as the running buffer using a 3%

agarose gel. The gel was run at 250 V for 45 min and was stained for 15 min in ethidium bromide. The tests were performed in duplicate or triplicate.

Preparation of Calcium Montmorillonite

Calcium montmorillonite (Ca-MMT) was prepared by mixing equal volumes of 1 M $CaCl_2$ with 6 mg/mL Na-MMT and centrifuging at 32,000 x g for 30 min at 4°C. The resulting pellet was subsequently washed with cold water three times and was resuspended in water to match the initial volume. Confirmation of successful recovery was performed by measuring the A_{230} of the MMT before and after treatment. Na-MMT and Ca-MMT suspensions were sonicated using a Sonics & Materials, Inc. Vibracell VC130 Sonicator. The clay was sonicated at an amplitude of 40 for 4 min.

Salt Competition and Displacement Assays for Calcium Montmorillonite

The salts that were used for these sets of experiments were sodium carbonate and sodium sulfate. For a typical competition assay, 4 μL RNA was mixed with 50 μL 6 mg/mL MMT plus salt to give 0 mM, 1 mM, 10 mM, 100 mM or 500 mM final concentrations of each salt in a total volume of 150 μL. The displacement assays were prepared using the same amounts of ssRNA, ddH_2O, MMT, and salt concentrations. However, the RNA, water, and MMT were mixed and incubated for 5 min first, before adding the salts, for the displacement assays. The binding reactions were shaken for 5 min and then centrifuged for 30 min at 21,000 xg. The A_{260} of each sample's supernatant was measured and the percentage of RNA bound calculated.

Effect of Heat and Sonication on Separation of Platelets of Calcium Montmorillonite

A solution of 2 mg/mL CaMMT was heated at 100°C for 5 min and immediately cooled in a wet ice bath and was labelled as HC-CaMMT. CaMMT (2 mg/ml) was sonicated for 3 min or 15 min at an amplitude of 50 and labelled as CaMMT Son t = 3 and CaMMT Son t = 15, respectively. Assays utilized 2 mg/mL of CaMMT or HC CaMMT or CaMMT Son t = 3 or CaMMT Son t = 15 combined with 6 µL ssRNA (1000 ng/µL) in a total volume of 150 µL. After letting the solutions sit for 5 min at RT, the solutions were then centrifuged for 1 h at 21,000 xg. The A_{260} of each sample's supernatant was measured and the percentage of RNA bound was calculated.

Electrophoretic Mobility Shift Assays for RNA:MMT Complexes

The EMSA gels were performed using 3.0-3.5% agarose gels and Horizon 11-14 gel rigs as described (52). Initial gels were prepared in 45-50 mL 0.5X TB (Tris-borate) buffer. Later, other electrophoresis buffers were tested, including 1X, 0.5X and 0.25X sodium borate (SB) and tricine/triethanolamine (30 mM/30 mM) as described (53-54). All samples were run at 300-350V for 5-10 min. SYBR Gold stock solution (10,000X) was diluted to 4X in 40 mL running buffer and layered onto the top of gels. Staining was performed for 15 min, followed by destaining for 20 min in gel buffer with shaking and photography using a Protein Simple Red Imaging System. Assays utilized 200 ng PvuRNA combined with 0.04, 1, 2.5, and 5 mg/mL Ca-MMT in a volume of 20 µL. After letting the solutions sit for 5 min at RT, 4 µL of 30% glycerol was added, followed by mixing and loading of 18 µL of each sample onto the gel.

CHAPTER III

RESULTS AND DISCUSSION

A major goal of this research was to analyze the association of small DNAs and RNAs with the naturally occurring nanotube halloysite. In addition, the current work has expanded upon the earlier work done by Blanca Rodriguez characterizing the interaction of RNAs with montmorillonite. We are specifically interested in assessing the binding affinity of small oligonucleotides to the clay HNT. The optical and sedimentation properties of HNT were investigated through spectroscopic analysis initially to ensure that the absorbance from HNT didn't contribute or affect the nucleic acid binding assays. For these types of assays to be quantitative, it is important that the ability of HNT particles to absorb or scatter light at 260 nm must be known. To quantitate the binding of HNT with oligonucleotides, HNT and DNA/RNA were incubated together and centrifuged to pellet the clay plus any DNA molecules that had adsorbed onto the HNT. The A_{260} of the supernatant was measured and presumed to represent the amount of DNA or RNA which has not bound to HNT. The wavelength 260 nm was chosen due to the fact that the DNA has strong absorbance at 260 nm (55-59).

To find out whether there is a significant difference in absorbance of halloysite particles when they are vacuumed or sonicated, spectroscopic measurements and scans of three different types of HNT (untreated, vacuumed and sonicated) at 100 µg/mL in ddH_2O were measured. Absorbance scans of 100 µg/mL of HNT are presented in Figure 8A. The scans revealed that there is no significant difference in apparent absorbances of untreated, vacuumed and sonicated HNT. All three sets showed increasing absorbance at lower wavelengths, with strongest absorbance at ultraviolet light wavelengths (200 – 400 nm).

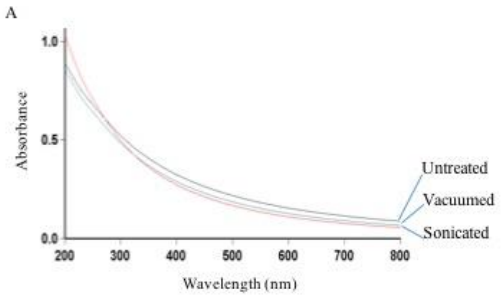

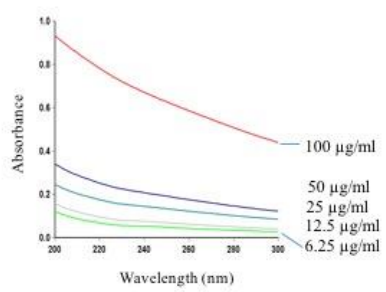

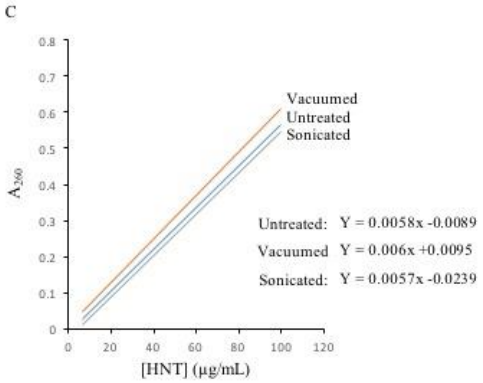

D

	Starting [HNT]	After Centrifugation		
		A_{260}	[HNT]	HNT Removed
Untreated HNT	1 mg/mL	0.0043	0.0023	99.8 %
	0.5 mg/mL	0.0037	0.0022	99.6 %
	0.25 mg/mL	0.0003	0.0016	99.4 %
Vacuumed HNT	1 mg/mL	0.0177	0.0014	99.9 %
	0.5 mg/mL	0.0057	-0.0006	100.1 %
	0.25 mg/mL	0.0087	-0.0001	100.1 %
Sonicated HNT	1 mg/mL	0.0717	0.0168	98.3 %
	0.5 mg/mL	0.0487	0.0127	97.5 %
	0.25 mg/mL	0.0370	0.0107	95.7 %

Figure 8. Optical and sedimentation properties of HNT. (A) Absorbance scan of 100 µg/mL HNT (untreated, vacuumed and sonicated) from 200 – 800 nm; (B) Absorbance scan of different concentrations of untreated HNT from 200 – 300 nm; (C) Absorbance of ultraviolet light (260 nm) by HNT solution follows Beer's Law; (D) The percentage of HNT precipitated at different concentrations of HNT at 30 min centrifugation time.

Halloysite (untreated, vacuumed and sonicated) samples (100 µg/mL, 50 µg/mL, 25 µg/mL, 12.5 µg/mL, and 6.25 µg/mL) were scanned from 200 – 300 nm and the results suggested that absorbances were concentration dependent (Figure 8B). Absorbance scan data were plotted into a best-fit trendline using Microsoft Excel in order to generate a Beer's Law plot (Figure 8C). From this data, it was observed that there is a consistent increase in the absorbance at 260 nm with increase in the concentration of HNT. The best-fit trend line indicated a concentration dependent increase in absorbance and the Beer's Law equations were used in a set of experiments to quantitate the sedimentation efficiencies of HNT.

For centrifugation experiments, three sets of each untreated, vacuumed and sonicated HNT solution at different concentrations (1 mg/mL, 0.5 mg/mL and 0.25 mg/mL) were prepared.

The solutions were centrifuged at 21,000 xg at 20ºC for 5 min, 15 min, 30 min or 60 min. After centrifugation, the supernatant was collected and the A_{260} was measured and converted to an HNT concentration using the equations derived in Figure 8C. The amount of HNT precipitated at different concentrations of HNT at 30 min centrifugation time is presented in Figure 8D. The data indicates that at the highest concentration, 1 mg/mL, a 30-min spin at 21,000 xg, at 20˚C was sufficient to sediment approximately 100% of the HNT. Sonicated HNT sedimentation (96-98%) was slightly less efficient than the untreated and vacuumed HNTs, which showed > 99% efficiency. It is possible that sonication caused breakage or separation of some particles that had been attached to each other, leading to a small fraction of smaller particles that did not sediment efficiently.

The next experiment tested the effect of incubating ssDNA 25mers with HNT (4 mg/mL) for different time periods. Three sets for each untreated, vacuumed and sonicated solution were incubated with shaking for different incubation times, i.e., 5 min, 15 min and 30 min. After incubation, the tubes were centrifuged at 25000 xg at 20ºC for 30 min. After centrifugation, 60 µL of supernatant was collected and the A_{260} was measured. The results suggested that after 15 min of shaking the binding of ssDNA to HNT remained the same (Figure 9). Also, sonication of HNT improved the binding of ssDNA to HNT slightly. The increased apparent binding of ssDNAs may be due to separation of aggregated HNT particles into individual tubes. This could possibly increase the surface area for interaction of ssDNAs with HNT.

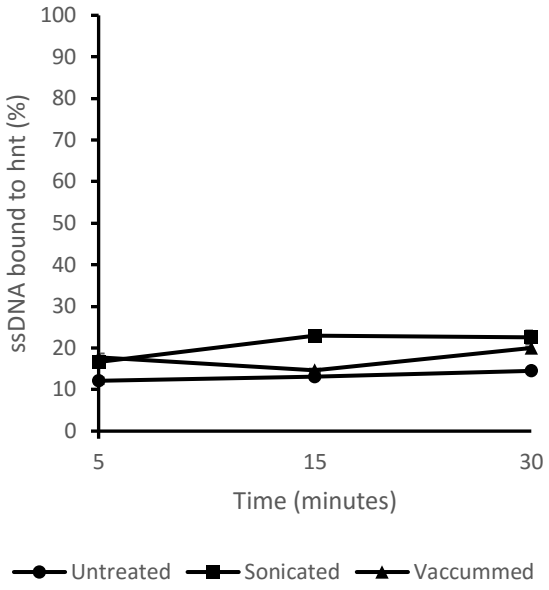

Figure 9. The percentages of ssDNA bound to HNT (4 mg/mL) at different incubation times.

The structures and sequences of oligonucleotides used in this study are presented in Figure 10.

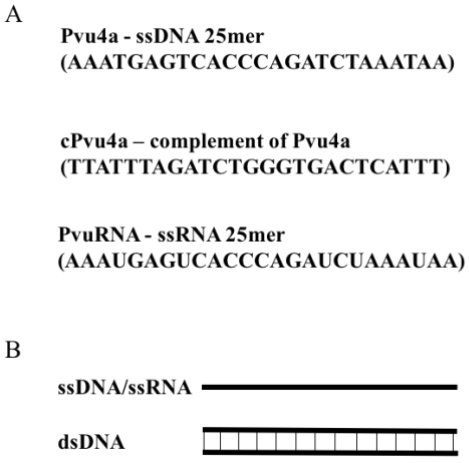

Figure 10. The sequences and structures of oligonucleotides used in the study.

Centrifugation binding assays using the best incubation and centrifugation parameters were employed to assess the adsorption of nucleic acids to HNT (60). The HNT-nucleic acid

mixtures were incubated for 15 min and centrifuged at 21,000 xg, at 20˚C for 30 min (Figure 11A). The amount of free nucleic acids versus those that adsorbed to the sedimented HNT was quantitated by measuring the absorbance of the supernatant at 260 nm after centrifugation. In the first set of experiments the ssDNA 25mers were mixed with increasing amounts of HNT. The percentages of DNA bound to vacuumed and unvacuumed/untreated HNT were compared against HNT concentration. The averages and standard deviations from three or four assays at each concentration of HNT are shown in Figure 11B. The results indicate that only a small fraction of ssDNA was bound to HNT. Vacuumed HNT bound ssDNA similar when compared with vacuumed HNT. At a high concentration of HNT (4 mg/mL) vacuumed HNT bound the DNA modestly better but with overlapping standard deviations. The next set of experiments were continued with untreated HNT (not vacuumed and not sonicated HNT), as vacuum didn't have much effect on binding of HNT to nucleic acids.

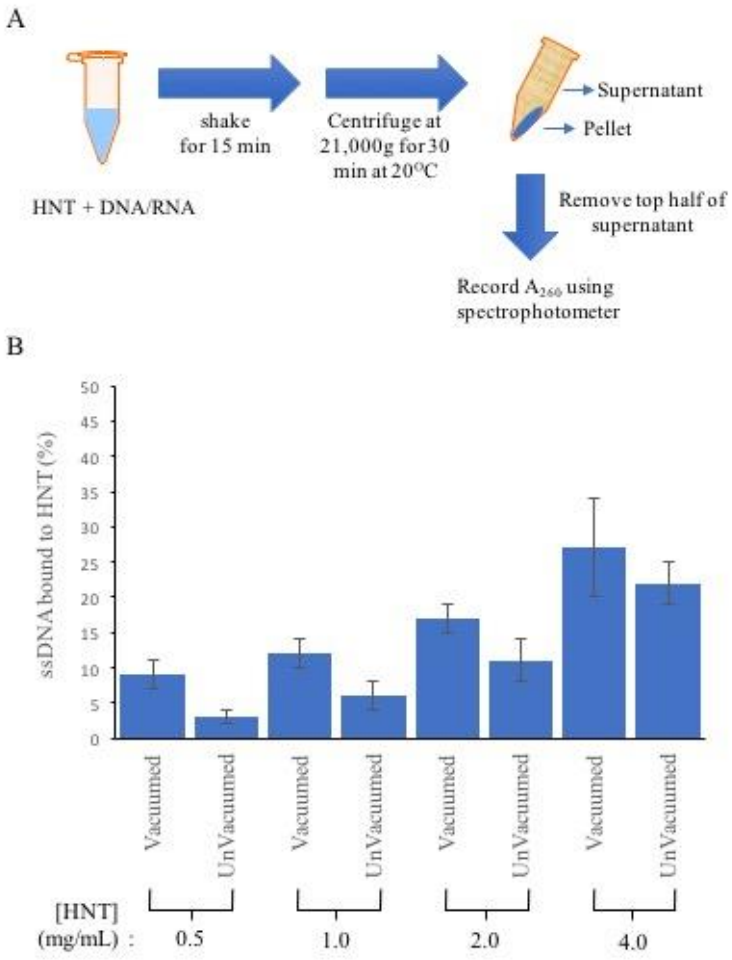

Figure 11. (A) Diagram illustrating the method used to investigate the affinity of HNT for small DNAs and RNAs; (B) Assessment of binding of ssDNA to vacuumed and unvacuummed HNT using centrifugation assays.

ssDNA, dsDNA and ssRNA 25mers were mixed with increasing concentrations of HNT and the percentages of nucleic acid bound were plotted against HNT concentration (Figure 12A). At the highest concentration of HNT, 4 mg/mL, ~46% of ssRNA was bound, but only ~25% of ssDNA and ~22% of dsDNA was bound (~2-fold difference). At lower concentrations of HNT, the binding efficiencies were all similar. The results indicate that the affinities of single-stranded and double-stranded DNA 25mers for HNT do not differ strongly from one another.

Modifying the HNT with cations could promote the binding of nucleic acids to HNT. Assays were performed with and without addition of salts such as NaCl and $MgCl_2$. The effect of

NaCl and $MgCl_2$ was demonstrated by adding 0, 1, 10, and 100 mM NaCl or $MgCl_2$ with 4 mg/mL HNT and ssDNA, dsDNA, or ssRNA 25mers (Figure 12B and 12C). With the addition of 100 mM NaCl, the binding increased to 63% for ssDNA, 53% for dsDNA and 90% for ssRNA. With the addition of 100 mM $MgCl_2$ the binding increased to 92% for ssDNA, 81 % dsDNA and 85% for ssRNA. Unlike Na^+ ions, addition of Mg^{2+} cations enhanced binding at concentrations as low as 1 mM (Figure 12C). This is reasonable, as magnesium has higher charge density than sodium and allows the HNT to bridge readily to DNA/RNA. NaCl increased binding moderately, but the addition of $MgCl_2$ significantly promoted the adsorption of all nucleic acids to HNT even at low concentrations of $MgCl_2$ (1 - 10 mM) (Figure 12C). Overall, these results suggest that 25mers have weak affinity for HNT, but the addition of metals, in particular Mg^{2+} at 1 mM or higher, drastically improves the adsorption of the RNA and DNA to HNT.

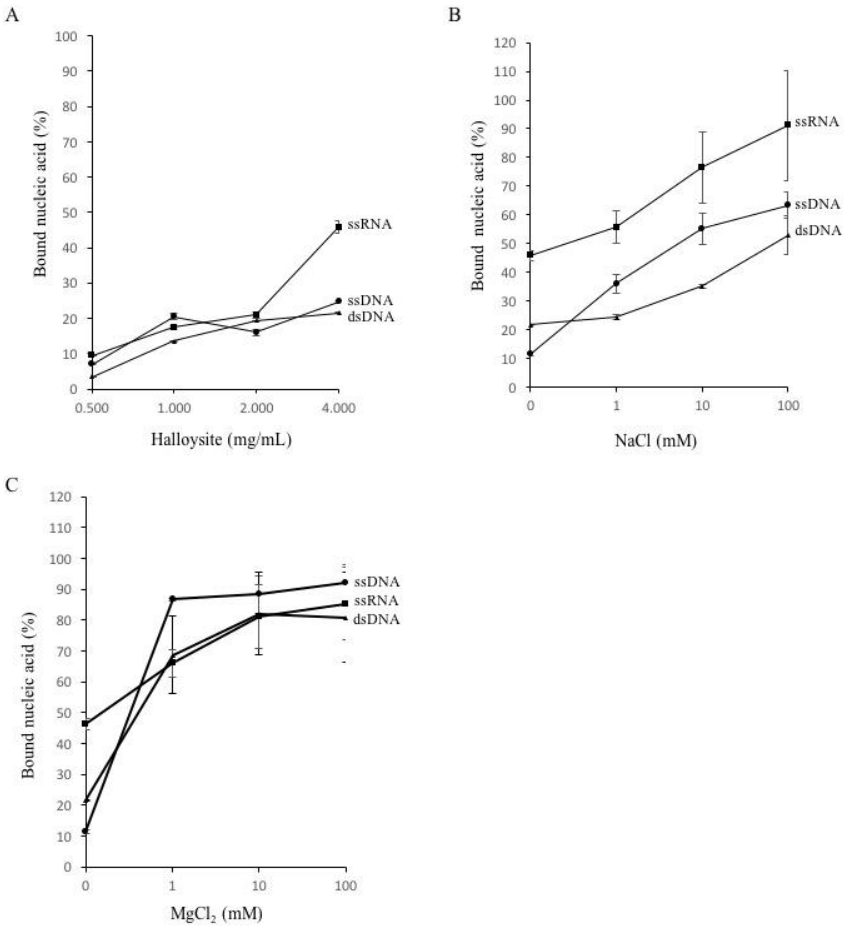

Figure 12. Assessment of binding of DNA and RNA to HNT using centrifugation assays: (A) The percentage of ssDNA, dsDNA and ssRNA bound at different concentrations of HNT; (B) The percentage of ssDNA, dsDNA and ssRNA bound at 4 mg/mL HNT with addition of increasing amount of NaCl; (C) The percentage of ssDNA, dsDNA and ssRNA bound at 4 mg/mL HNT with addition of increasing amount of $MgCl_2$.

HNT-DNA-Nuclease Experiment

To evaluate protection of DNA from nuclease digestion by HNT and to potentially demonstrate the adsorption of the nucleic acids into the lumen, nuclease protection experiments were performed. DNase I was used as the nuclease. DNase I is an endonuclease that degrades or breaks DNA into smaller fragments. It does so by cleaving or hydrolyzing the phosphodiester bonds holding the pentose sugars to the phosphate group in the DNA's backbone.

Figure 13A illustrates the possible outcomes of digestion of DNA with DNase I. If DNA is bound to the surface, it should be degraded but if its inside the lumen it should be protected. Two tubes containing HNT – ssDNA complex mixture in the presence of $MgCl_2$ (100 mM) were prepared as described earlier. To one of the tubes DNase I was added and the other was used as control to compare the effect of DNase I. Then DNA was recovered by the method described earlier. The recovered DNA was run on a 3% agarose gel using 0.5X TB buffer at 250 V for 45 min. The gel assay demonstrated that the association of ssDNA with HNT protected it from digestion by DNase I (Figure 13B). The absence of a band for ssDNA in the presence of nuclease (the third lane in the gel) indicates that the bonds between nucleotides in ssDNA were broken and the structure of ssDNA was destroyed by nuclease. The presence of a band in the lane for HNT/ssDNA + Nuclease (the last lane on the right) indicates that the nuclease enzyme was not associated with ssDNA and the ssDNA was not degraded, being protected due to its association with HNT. The gel assay suggests that the DNA entered into the lumen and bound to the inner walls of HNT, where it was inaccessible to the nuclease enzyme. The idea that DNA is binding inside the lumen of HNT can be also supported with reference to a mica experiment (61). Mica is an aluminosilicate mineral clay similar to HNT that occurs in sheet-like structures. In a previous mica experiment, short segments of DNA were allowed to bind to a mica surface. Then the mica-bound DNAs were exposed to DNase I. Later the resulting fragments were separated by electrophoresis. Though the DNase I enzyme was bulky, it was still able to cleave the phosphodiester bonds on the DNA. Similarly, in the HNT/ssDNA + Nuclease experiment, if DNA was bound outside it would have been cleaved by the nuclease enzyme into smaller fragments and the recovered DNA would not have shown only the original, intact band on the gel.

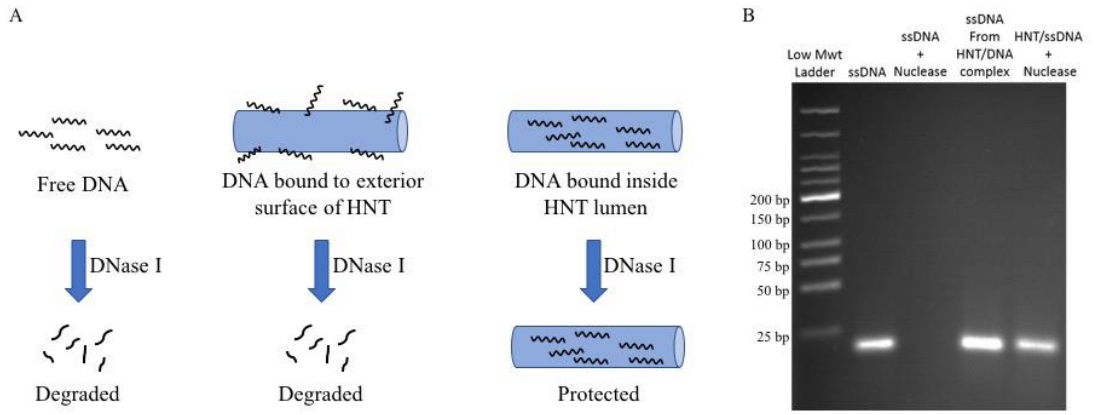

Figure 13. Investigation of the susceptibility of HNT-bound DNA to digestion with the DNase I. (A) Assessment of nature of ssDNA bound to HNT in presence of nuclease; (B) Gel demonstrating protection of bound ssDNA by HNT when treated with nuclease DNase I.

Use of Sonication and Heat to Increase Nanoparticle Surface Area

Experiments were performed in an effort to increase the surface area available for binding of RNA molecules to CaMMT. Blanca Rodriguez's studies showed that CaMMT clay had better binding affinity towards small nucleotides in absence of metal cations when compared to NaMMT, so CaMMT was chosen for the following experiment. CaMMT was heated at 100˚C for 5 min to break the tactoids of CaMMT and immediately cooled in an ice bath. In a separate experiment, CaMMT was sonicated for 3 min or 15 min at an amplitude of 50 to separate the CaMMT into individual platelets and increase the surface area, potentially increasing the binding of RNA to CaMMT (Figure 14A). There was not much difference in the percentage of ssRNA bound to unheated CaMMT, sonicated CaMMT and heated-and-cooled CaMMT (Figure 14B). The results suggest that these methods were not able to separate the CaMMT into individual platelets and increase the surface area.

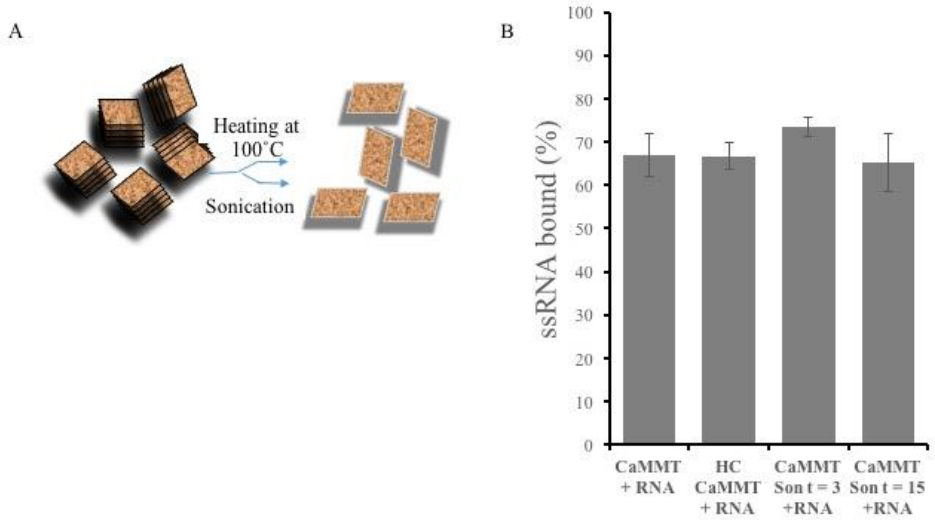

Figure 14. (A) Schematic representation of tests performed to determine if heating or sonication of CaMMT could separate them into individual platelets; (B) Comparison of the percentage of ssRNA bound to unheated CaMMT, sonicated CaMMT and heated-and-cooled CaMMT.

MMT Salt Competition Assays and Displacement

Concern about anions displacing or competing with the RNA for binding to CaMMT *in vitro* or inside cells led us to conduct a series of centrifugation binding assays with two distinct anions, sodium carbonate (Na_2CO_3), and sodium sulfate (Na_2SO_4). Competition assays were performed that involved simultaneously mixing 6 mg/mL CaMMT with ssRNA and increasing concentrations of sodium carbonate or sodium sulfate at 1, 10, or 100 mM. The percentage of RNA remaining unbound in the presence and absence of other anions was plotted against the concentration of salt added (Figure 15). At the highest concentration of 100 mM, carbonate ions reduced RNA binding from approximately 60% to 10% (Figure 15A). Sulfate was less effective, reducing bound RNAs to only 40% at 10 and 100 mM (Figure 15B). Displacement studies were performed in a similar manner, except that the anions were added last to the ssRNA-CaMMT mixture, after RNA-CaMMT complexes had already formed. These experiments also revealed a larger effect for carbonate ions, which reduced the fraction of bound RNAs from 70% to 30% at

100 mM Na_2CO_3 (Figure 15C and 15D). These experiments show that while anions such as carbonate and sulfate can indeed be exchanged for RNA, the process is inefficient, even at very high concentrations of the anions. This could be explained by the fact that it is difficult for small molecules to displace a large molecule that is attached at multiple sites. Carbonate was better at competing than sulfate. This could be possibly explained by the stability and solubility of carbonate and sulphate ion. Carbonate was better at competing than sulfate. This could be possibly explained by the stability and solubility of carbonate and sulphate ion. By analogy in nature large deposits of calcium carbonate exist as limestone while calcium sulfate hydrates, gypsum, although also common are not as common as limestones. Calcium carbonates are far less soluble than gypsum.

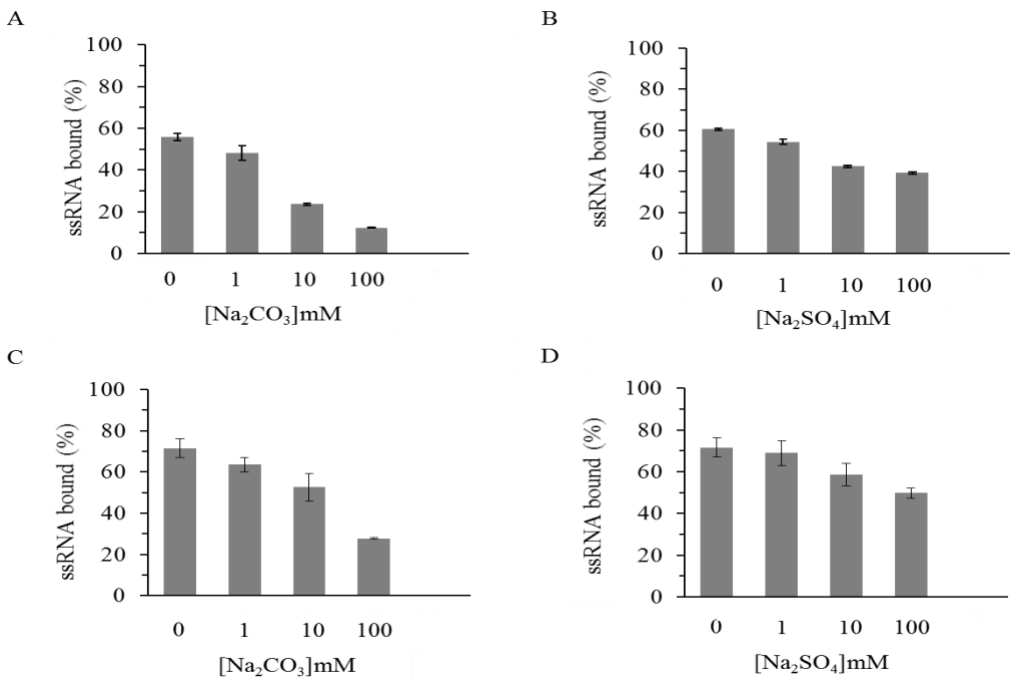

Figure 15. Centrifugation assays performed with ssRNA 25mers (A_{260} ~1.0), 6 mg/mL CaMMT, and the addition of sodium carbonate (Na_2CO_3) or sodium sulfate (Na_2SO_4) at 0, 1, 10, or 100 mM. (A) Centrifugation assays were performed to determine the ability of carbonate to compete with ssRNA for CaMMT binding. (B) Centrifugation assays were performed to determine the ability of sulfate to compete with ssRNA for CaMMT binding. (C) Displacement of RNA from CaMMT after adding carbonate to the solution was also analyzed. (D) Displacement of RNA from CaMMT after adding sulfate to the solution was also analyzed.

Electrophoretic Mobility Shift Assay of RNA-montmorillonite Complexes

In a previous study of the interactions of DNAs and RNAs with the nanoclay hydrotalcite (62), an electrophoretic mobility shift assay (EMSA) system for analysis of binding was developed. In the most common application of this biochemical assay, increasing amounts of a DNA or RNA binding protein are mixed with a set amount of nucleic acid, followed by an incubation period to allow binding to occur (63-64). The products of each binding reaction are then run in different lanes of a gel, separating the molecules by size, and the nucleic acid bands are visualized. Unbound nucleic acid migrates quickly and produces a single band low in the gel. As the protein concentration is increased, some of the nucleic acid molecules become bound and a new slower-migrating band usually appears higher up in the gel that represents the protein:nucleic acid complex. Sometimes multiple complexes of different sizes are formed that do not produce a single discrete upper band. The process can be monitored by analyzing the formation of the new band(s) or the progressive loss of the lower, free nucleic acid band. We employed 3.5% agarose gels to analyze complexes formed between Ca-MMT and RNA by following the parameters set forth previously (65-66). The gels were run at high voltage (250-300 volts with 14 cm long gels) for 5-10 minutes using 0.5X TB (Tris-borate) buffer and stained using SYBR Gold as described (67). The SYBR Gold stained the RNA but not the clay, allowing visualization of the free RNA band as it migrated down the gel. As an initial control experiment, we performed a hydrotalcite electrophoretic mobility shift assay. In the assay PvuRNA was mixed with increasing amounts of the nanoclay hydrotalcite (HT), incubated at RT for 10 min, and analyzed using EMSAs. A progressive loss of the free RNA band was observed as clay concentration was increased from 0.04 mg/mL to 0.64 mg/mL (Figure 16A). When the same

experiment was performed using PvuRNA and Ca-MMT at concentrations between 0.4 and 5.0 mg/mL, no progressive reduction of band intensity was seen for the ssRNA (Figure 16B) suggesting that the MMT-RNA complexes were not stable under these conditions. The 45 mM Tris in the electrophoresis buffer is an amine that can potentially bind strongly to the MMT particles (68-69), so the experiment was repeated using other electrophoresis media in an effort to find one that did not destabilize the complexes. Examples of this approach are shown in Figure 16C and 16D, where 1X and 0.25X sodium borate (SB) solutions were used (70). No stable Ca-MMT:RNA complexes could be detected using this non-Tris buffer. Several other attempts were made to improve the stability of the complexes, including using other weak acid:weak base buffers described by Liu et al., (71) adding divalent metals to the electrophoresis buffer and gel, and running the gels at lower voltages to slow migration (data not shown), but the MMT:RNA complexes remained labile under all conditions tested.

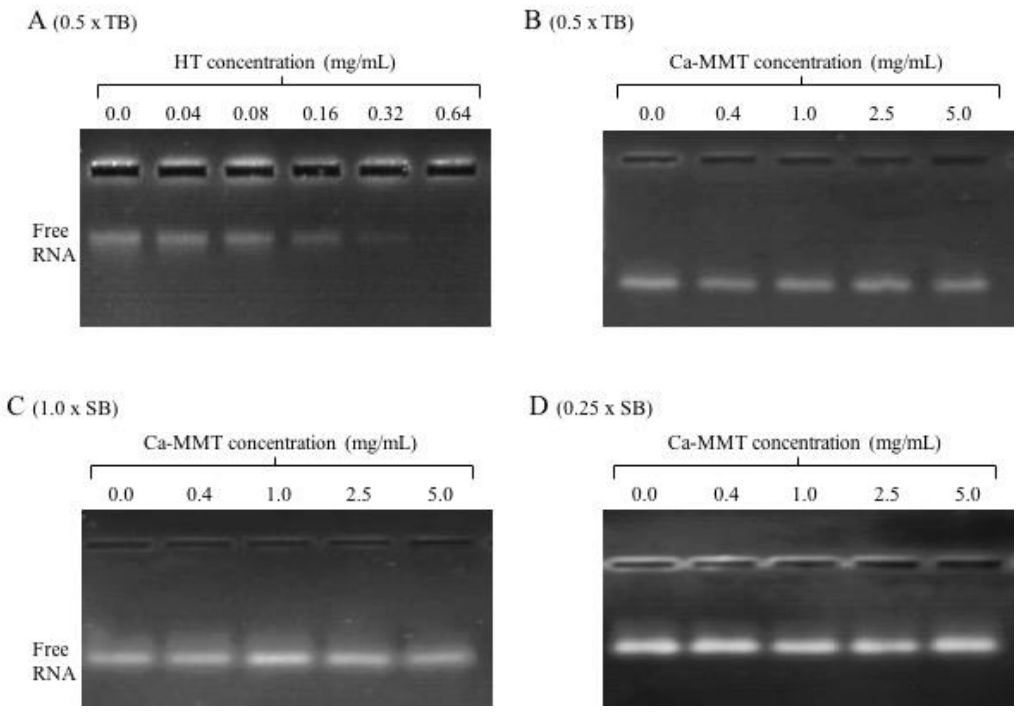

Figure 16. Electrophoretic mobility shift assays can readily monitor formation of RNA:HT complexes but not RNA:Ca-MMT complexes. Assays were performed using 3.5% agarose gels and ssRNA 25mer PvuRNA. (A) Addition of increasing amounts of hydrotalcite (HT) to 200 ng ssRNA leads to disappearance of the free RNA band as HT:RNA complexes are formed. (B-D) In contrast to results with HT, MMT:RNA complex formation could not be monitored using conventional Tris-borate (TB) or other electrophoresis buffers such as sodium borate (SB).

CHAPTER IV

SUMMARY AND CONCLUSIONS

In the current study, we have analyzed the affinity of halloysite for small nucleic acids including ssDNA, dsDNA and ssRNA. Results of these experiments can be used to develop improved assays for quantitating the binding of larger nucleic acids to clay surfaces. The approach used here can be generally applicable to study the interaction of nanoclays with many other biomolecules and biopolymers. Spectrophotometric scanning of three types of HNT revealed that there is no statistically significant difference in UV absorbance when HNT is vacuumed or sonicated. HNT was vacummed to remove the trapped gases. Sonication of HNT was done in order to separate the HNT into individual tubes. The absorbance and centrifugation assays of HNT-nucleic acid complexes revealed that HNT has very low natural affinity for these biomolecules. Addition of salts increased the binding of DNA and RNA to HNT. This effect was achieved with magnesium ions even at low concentrations. These observations are consistent with previous studies that demonstrated that divalent cations can promote association of some clays with DNA(72-74).

Studies have demonstrated that planar (flat) clay minerals such as illite, montmorillonite and kaolinite protect DNA against nucleases (75-77). In this study agarose gel electrophoresis was used to investigate whether DNA adsorbed onto HNT was protected from degradation by DNase I. The results suggested that the adsorption of DNA on HNT provides protection against nucleases. Two hypotheses can be proposed to explain this mechanism. First, the DNA may be entering into the lumen of HNT and binding to the inner walls of the tube where it cannot be accessed by DNase I. An alternative hypothesis could be adsorption of the DNA onto the surface of HNT, but it is not digested by the nuclease when bound. This second hypothesis is unlikely

because past studies have demonstrated that DNA bound to mica surfaces is cut by DNase I (61). Mica is an aluminosilicate clay similar to kaolinite and HNT. This idea could be supported by the fact that the activity of enzyme is reduced when bound to other molecules (78-83). Halloysite has been demonstrated as a potential vector for gene delivery with applications in cancer treatment (84-86). The research done here can contribute and support use of halloysite in the field of biomedicine.

Many past studies have focused on understanding the role of homoionic montmorillonite in the origins of life, with most studies focused on interactions with DNA (87). Past studies that looked at the association of RNA with MMT produced several results with potential evolutionary importance, e.g., the demonstration that MMT can protect and help catalyze the polymerization of RNA from activated mononucleotides (88-90). However, there has not been much focus on probing MMT as a carrier for RNA molecules for therapeutic purposes.

The interaction of MMT with RNA has been little explored and previous work has focused on interaction with mononucleotide components rather than long strands of RNA (91-93). The current work on montmorillonite has expanded upon the earlier work done by Blanca Rodriguez. Adsorption studies using RNA and montmorillonite (Na-MMT and Ca-MMT) in the presence of cations such as Na^+ and Mg^{2+}were performed by Blanca Rodriguez. In the current study, we assessed the strength of the interaction between small RNAs and Ca-MMT using anion competition and displacement experiments. Sulfate ions were largely ineffective in these assays. However, carbonate ions showed competitive and displacement activity, albeit only at high concentrations (100 mM). These data suggest that binding of RNAs to the clay is not likely to be disrupted significantly by the presence of small anions in complex solutions *in vitro* or *in vivo*. Although interactions between RNAs and the synthetic clay hydrotalcite could readily be

monitored using mobility shift assays (Figure 16A) (94), we were unable to assess RNA:montmorillonite complex formation using this method. Several changes were made to the electrophoresis gels and conductive media, including elimination of buffer components such as Tris known to interact with MMT (95-96) and addition of Mg^{2+} ions to the gel and electrophoresis buffer, but no loss of free RNA or gain of shifted higher molecular weight bands could be detected. It is unclear why the MMT complexes were so labile during electrophoresis. One possibility is that the clay and RNA have opposite charges and are drawn in different directions during electrophoresis, disrupting the complexes. However, we have observed that MMT can be loaded onto and separated on agarose gels, where it retains a net negative charge in standard TAE and TBE electrophoresis buffers (pH 7.5-8.0) and migrates toward the positive electrode, similar to RNA and DNA (the clay particles were visualized by staining with methylene blue; LKL and GWB, unpublished).

Future work could include experiments to confirm the site of binding of DNA onto HNT by tagging DNA molecules with a fluorescent group and looking at them by using a confocal microscope. Other possible experiments could include demonstrating release of DNA bound to HNT back into the cell.

REFERENCES

1) DeLong, R. K.; Akhtar, U.; Sallee, M.; Parker, B.; Barber, S.; Zhang, J.; and Engstrom, *E. Biomaterials*, 2009. 30, 6451-6459.

2) Carter, P. J.; and Samulski, R. J. *International journal of molecular medicine*. 2000. 6, 17-28.

3) Rubanyi, G. M. *Molecular aspects of medicine*. 2001. 22, 113-142.

4) Wivel, N. A.; and Wilson, J. M. *Hematology/oncology clinics of North America*. 1998. 12(3), 483-501.

5) El-Aneed, A. *European journal of pharmacology*. 2004. 498, 1-8.

6) Thrasher, A. J.; Gaspar, H. B.; Baum, C.; Modlich, U.; Schambach, A.; Candotti, F.; and Blyth, K. *Nature*. 2006. 443, E5-E6.

7) Rubanyi, G. M. *Molecular aspects of medicine*. 2001. 22, 113-142.

8) Giacca, M. *Gene therapy*. 2010. 47-137.

9) Sokolova, V.; and Epple, M. *Angewandte Chemie*. 2008. 47: 1382 – 1395.

10) Wilczewska, A. Z.; Niemirowicz, K.; Markiewicz, K. H.; and Car, H. *Pharmacological Reports*. 2012. 64, 1020-1037.

11) De Jong, W. H.; and Borm, P. J. A. *International Journal of Nanomedicine*. 2008. 3: 133-149.

12) Suresh, R.; Borkar, S. N.; Sawant, V. A.; Shende, V. S.; and Dimble, S. K. *International Journal of Pharmaceutical Sciences and Nanotechnology*. 2010. 3: 901 – 905.

13) Choy, J. H.; Choi, S. J.; Oh, J. M.; and Park, T. *Applied Clay Science*. 2007. 36, 122-132.

14) Aguzzi, C.; Cerezo, P.; Viseras, C.; and Caramella, C. *Applied Clay Science*. 2007. 36, 22-36.

15) Beall, G. W.; Sowersby, D. S.; Roberts, R. D.; Robson, M. H.; and Lewis, L. K. *Biomacromolecules*. 2008. 10, 105-112.

16) Sanderson, B. A.; Sowersby, D. S.; Crosby, S.; Goss, M.; Lewis, L. K.; and Beall, G. W. *Biointerphases*. 2013. 8, 8.

17) Lin, F. H.; Chen, C. H.; Cheng, W. T.; and Kuo, T. F. *Biomaterials*. 2006. 27, 3333-3338.

18) Calabi floody marcela, M.; Theng benny, k.; Ryes, Patricio.; and Mora gil maria de la, l. *Natural nanoclays*. 2004.

19) Clay—Columbia Encyclopedia Article about Clay < www.columbia.thefreedictionary.com>

20) Clay Minerals—Sci-Tech Encyclopedia <www.answers.com>.

21) Montmorillonite < www.en.wikipedia.org>.

22) Mineral Gallery—The Phyllosilicate Subclass < www.mineral.galleries.com>.

23) Building the phyllosilicates <http://pubpages.unh.edu/~harter/crystal.htm>.

24) Mitchell, J. K.; and Soga, K. John Wiley and Sons, New York. 2005.

25) Anon. Cation Exchange Capacity <www.css.cornell.edu>.

26) Du, M.; Guo, B.; and Jia, D. *Polymer International*. 2010. 59, 574-582.

27) Abdullayev, E.; and Lvov, Y. *Journal of materials chemistry*. 2013. 1, 2894-2903.

28) Levis, S. R.; and Deasy, P. B. *International Journal of Pharmaceutics*. 2002. 243, 125-134.

29) Abdullayev, E.; and Lvov, Y. *Journal of materials chemistry*. 2013. 1, 2894-2903.

30) Guimaraes, L.; Enyashin, A. N.; Seifert, G.; and Duarte, H. A. *The Journal of Physical Chemistry C*. 2010. 114, 11358-11363.

31) Halloysite Clay Nanotubes < http://phantomplastics.com/functional-fillers/halloysite/>.

32) Cadene, A.; Durand-Vidal, S.; Turq, P.; and Brendle, J. *Journal of Colloid and Interface Science*. 2005. 285, 719-730.

33) Helmy, A. K.; Ferreiro, E. A.; and De Bussetti, S. G. *Journal of colloid and interface science*. 1999. 210, 167-171.

34) Aguzzi, C.; Sandri, G.; Cerezo, P.; Carazo, E.; and Viseras, C. *Nanosized Tubular Clay Minerals*. 2016.708-725.

35) Elumalai, D. N.; Lvov, Y.; and Derosa, P. *Journal of Encapsulation and Adsorption Sciences*. 2015. 5, 74.

36) Kommireddy, D. S.; Ichinose, I.; Lvov, Y. M.; and Mills, D. K. *Journal of Biomedical Nanotechnology*. 2005. 1, 286-290.

37) Vergaro, V.; Abdullayev, E.; Lvov, Y. M.; Zeitoun, A.; Cingolani, R.; Rinaldi, R.; and Leporatti, S. *Biomacromolecules*. 2010. 11, 820-826.

38) Verma, N. K.; Moore, E.; Blau, W.; Volkov, Y.; and Babu, P. R. *Journal of Nanoparticle Research*. 2012. 14, 1-11.

39) Campos, V. F.; de Leon, P. M. M.; Komninou, E. R.; Dellagostin, O. A.; Deschamps, J. C.; Seixas, F. K.; and Collares, T. *Theriogenology*. 2011. 76, 1552-1560.

40) Shi, Y. F.; Tian, Z.; Zhang, Y.; Shen, H. B.; and Jia, N. Q. *Nanoscale research letters*. 2011. 6, 1.

41) Franchi, M.; Bramanti, E.; Bonzi, L. M.; Orioli, P. L.; Vettori, C.; and Gallori, E. *Origins of Life and Evolution of the Biosphere*. 1999. 29, 297-315.

42) Beall, G. W.; Sowersby, D. S.; Roberts, R. D.; Robson, M. H.; and Lewis, L. K. *Biomacromolecules*. 2008. 10, 105-112.

43) Franchi, M.; Ferris, J. P.; and Gallori, E. *Origins of Life and Evolution of the Biosphere*. 2003. 33, 1-16.

44) Lin, F. H.; Chen, C. H.; Cheng, W. T.; and Kuo, T. F. *Biomaterials*. 2006. 27, 3333-3338.

45) Blanca V.R.; Jorge, P.; Nicole. P.; Beall, G.W.; Corina, M.; and Lewis, L.K. *Biointerphases*. 2015.

46) Sambrook, J.; and Russell, SW. *Cold Spring Harbor Laboratory Press*; 2001.

47) Andersen, J. B.; C. Sternberg.; L. K. Poulsen.; S. P. Bjorn.; M. Givskov.; and S. Molin. *Microbiol*. 1998. 64, 2240-2246.

48) Borden, D.; and R. F. Giese. *Clays Clay Miner*. 2001. 49, 444-445.

49) Cai, P.; Q. Huang.; X. Zhang.; and H. Chen. *Soil Biol. Biochem*. 2006. 38, 471-476.

50) Crecchio, C.; and Stotzky, G. *Soil Biol. Biochem*. 1998. 30, 1061-1067.

51) Khanna, M.; and Stotzky, G. *Appl. Environ. Microbiol*. 1992. 58, 1930-1939.

52) Sanderson, B.A.; Araki,N.; Lilley, J.L.; Guerrero, G.; and Lewis, L.K.A *Analytical biochemistry*. 2014. 454, 44-52.

53) Liu, Q.; Li, X.; and Sommer, S.S. *Anal. Biochem*. 1999. 270, 112-122.

54) Brody, J.R.; and Kern, S.E. *Biotechniques*. 2004. 36, 214-217.

55) Franchi, M.; Bramanti, E.; Bonzi, L. M.; and Gallori, E. *Orig Life Evol Biosph*. 1999. 29, 297–315.

56) Lin, F. H.; Chen, C. H.; Cheng, W. T.; and Kuo, T. F. *Biomaterials*. 2006. 27, 3333–3338.

57) Pietramellara, G.; Franchi, M.; Gallori, E.; and Nannipieri, P. *Biol Fertil Soils*. 2001. 33, 402–409.

58) Khanna, M.; Yoder, M.; Calamai, L.; and Stotzky, G. *Sci Soils*. 1998. 3, 1–10.

59) Banin, A.; Lawless, J. G.; Mazzurco, J.; Church, F. M.; Margulies, L.; Orenberg, *J. B. Orig Life Evol Biosph*. 1985. 15, 89 –101.

60) Beall, G. W.; Sowersby, D. S.; Roberts, R. D.; Robson, M. H.; and Lewis, L. K. *Biomacromolecules*. 2009. 10, 105.

61) Rhodes, D.; and Klug, A. *Nature*. 1981. 5821, 378-80.

62) Rodriguez, B.V.; Pescador, J.; Pollok, N.; Beall, G.W.; Maeder, C.; and Lewis, L.K. *Biointerphases*. 2015. 10, 041007.

63) Rodriguez, B.V.; Pescador, J.; Pollok, N.; Beall, G.W.; Maeder, C.; and Lewis, L.K. *Biointerphases*. 2015. 10, 041007.

64) Ream, J.A.; Lewis, L.K.; and Lewis, K.A. *Anal. Biochem*. 2016. 511, 36-41.

65) Sanderson, B.A.; Araki, N.; Lilley, J.L.; Guerrero, G.; and Lewis, L.K. *Analytical biochemistry*. 2014. 454, 44-52.

66) Rodriguez, B.V.; Pescador, J.; Pollok, N.; Beall, G.W.; Maeder, C.; and Lewis, L.K. *Biointerphases*. 2015. 10, 041007.

67) Ream, J.A.; Lewis, L.K.; and Lewis, K.A. *Anal. Biochem*. 2016. 511, 36-41.

68) Saeki, K.; Kunito, T.; and Sakai, M. *Microbes Environ*. 2011. 26, 88-91.

69) Keren, R.; and O'connor, G.A. *Clays Clay Miner*. 1982. 30, 341-346.

70) Brody, J.R.; and Kern, S.E. *Biotechniques*. 2004. 36, 214-217.

71) Liu, Q.; Li, X.; and Sommer, S.S. *Anal. Biochem*. 1999. 270, 112-122.

72) Paget, E.; Monrozier, L. J.; and Simonet, P. *Microbiology Letters*. 1992. 97, 31–40.

73) Cai, P.; Huang, Q.; and Zhang, X. *Appl Clay Sci*. 2006. 32, 147–152.

74) Franchi, M.; Ferris, J. P.; and Gallori, E. *Orig Life Evol Biosph*. 2003. 33, 1–16.

75) Blum, S. A. E.; Lorenz, M. G.; and Wackernagel, W. *Syst. Appl. Microbiol*. 1997. 20, 513–521.

76) Ivarson, K. C.; Schnitzer, M.; and Cortez. *J. Plant Soil*. 1982. 64, 343–353.

77) Lorenz, M. G.; and W. Wackernagel. *Gene transfers and environment*. 1992. 103–113.

78) Davet, P. *INRA*. 1996. 6, 1968.

79) Khanna, M.; and Stotzky, G. *Appl. Environ. Microbiol*. 1992. 58, 1930–1939.

80) Lorenz, M. G.; and W. Wackernagel. *Gene transfers and environment*. 1992. 103–113.

81) Quiquampoix, H.; Abadie, J.; Baron, M. H.; Leprince, F.; MatumotoPintro, P.T.; Ratcliffe, R. G.; and Staunton, S. *American Chemical Society*. 1995. 321–333.

82) Sarkar, J. M.; Leonowicz, A.; and Bollag. J. M.; *Soil Biol. Biochem*. 1989. 21, 223–230.

83) Stotzky, G. *Soil Science Society of America*. 1986. 305–428.

84) Kawase, M.; Hayashi, Y.; Kinoshita, F.; Yamato, E.; Miyazaki, J.; Yamakawa, J.; Ishida, T.; Tamura, M.; and Yagi, K. *Biol Pharm Bull*. 2004. 27, 2049–2051.

85) Lin, F. H.; Chen, C. H.; Cheng, W. T.; and Kuo, T. F. *Biomaterials*. 2006. 27, 3333–3338.

86) Shamsi, M. H.; and Geckeler, K. E. *Nanotechnology*. 2008. 9, 1–5.

87) Franchi, M.; Ferris, J. P.; and Gallori, E. *Orig Life Evol Biosph*. 2002. 33, 1-16.

88) Franchi, M.; Ferris, J. P.; and Gallori, E. *Orig Life Evol Biosph*. 2002. 33, 1-16.

89) Hashizume, H.; Van der Gaast, S.; and Theng, B. K. G. *Evol Biol*. 2013. 61-78.

90) Ferris, J. P. *Elements*. 2005. 1, 145-149.

91) Hashizume, H.; Van Der Gaast, S.; and Theng, B.K.G. *Clay Minerals*. 2010. 45, 469-475.

92) Mignon, P.; Ugliengo, P.; and Sodupe, M. *Journal of Physical Chemistry C*. 2009. 113, 13741-13749.

93) Perezgasga, L.; Diaz, A.S.; Mendonza, A.N.; Gala, L.D.P.; and Mosqueira, F.G. *Origins of Life and Evolution of the Biosphere*. 2005. 35, 91-110.

94) Rodriguez, B.V.; Pescador, J.; Pollok, N.; Beall, G.W.; Maeder, C.; and Lewis, L.K. *Biointerphases*. 2015. 10, 041007.

95) Saeki, K.; Kunito, T.; and Sakai, M. *Microbes Environ*. 2011. 26, 88-91.

96) Keren, R.; and O'connor, G.A. *Clays Clay Miner*. 1982. 30, 341-346.